CONEM 2010
VI Congresso Nacional de Engenharia Mecânica

ABCM COMPROMETIDA COM A PROMOÇÃO DO DESENVOLVIMENTO DA ENGENHARIA E DAS CIÊNCIAS MECÂNICAS
ASSOCIAÇÃO BRASILEIRA DE ENGENHARIA E CIÊNCIAS MECÂNICAS

VI CONGRESSO NACIONAL DE ENGENHARIA MECÂNICA
VI NATIONAL CONGRESS OF MECHANICAL ENGINEERING
18 a 21 de agosto de 2010 – Campina Grande – Paraíba - Brasil
August 18 – 21, 2010 – Campina Grande – Paraíba – Brazil

MODELLING OF STICK-SLIP AND BIT-BOUNCE IN DRILL-STRING DYNAMICS VIA SMOOTHEN FUNCTIONS

Sandor Divenyi[1], ***sandord@yahoo.com.br***
Marcelo A. Savi[1], ***savi@mecanica.ufrj.br***
Marian Wiercigroch[2], ***m.wiercigroch@abdn.ac.uk***
Ekaterina Pavlovskaia[2], ***e.pavlovskaia@abdn.ac.uk***

[1] Universidade Federal do Rio de Janeiro
COPPE – Department of Mechanical Engineering
21.941.972 – Rio de Janeiro – RJ, Brazil, P.O. Box 68.503

[2] University of Aberdeen
Centre for Applied Dynamics Research, School of Engineering
AB243UE, Aberdeen, UK

Abstract: *In this work we model and analyse drill-string vibrations. A special attention is given to the transitions between different phases of motion, which for stick-slip and bit-bounce are normally treated as the non-smooth dynamics. Here we adopt smooth functions which are advantageous in terms of mathematical description and numerical analysis. Our studies have shown that the developed mathematical model is capable of predicting a full range of dynamic responses including the non-smooth behaviour.*

Keywords: *Nonlinear dynamics, stick-slip, drill bounce, drill-string.*

1. INTRODUCTION

Non-smooth behaviour occurs in many engineering systems. Some of such phenomena as chatter and squeal cause serious problems in many industrial applications and, in general, these forms of vibrations are undesirable because of their detrimental effects on the operation and performance of engineering systems. Mathematical modelling and numerical simulation of non-smooth systems present difficulties concerning an accurate detection of non-smoothness and then a robust switch from one set of equations to another. This makes their description cumbersome. Moreover, the dynamical responses of such systems are complex including chaos (Savi *et al.*, 2007; Pavlovskaia *et al.*, 2001; Andreaus & Casini, 2001; Hinrichs *et al.*, 1998)

Oil and gas drilling is an engineering process during which a wellbore is created. The fundamental part of the drilling rig is a drill-string which during the drilling experiences dangerous vibrations. A drill-string can be modelled as a non-smooth system by considering contact and non-contact with rock phases during operation. Basically, the drill-string vibrations can be classified into three different modes: axial, torsional and flexural vibrations. The coupling among these modes is essential in order to describe some important phenomena during drilling (Silveira & Wiercigroch, 2009; Christoforou & Yigit, 2003; Franca & Weber, 2004).

The main objective of this research is to undertake nonlinear dynamics analysis of a drill-string by considering it as a smoothen non-smooth system. An axial-torsional coupling allows to describe complex responses including stick-slip and bit-bounce. The mathematical model applies a smoothened switch model, which describes a non-smooth system with different sets of ordinary differential equations. The smoothened system is built by defining the transition equations of motions that govern the dynamical response during the transition from one set to another. Therefore, the state space is divided into subspaces that have their own smooth ordinary differential equations. The undertaken numerical simulation confirms that stick-slip and bit-bounce can be modelled effectively with the smoothen functions. It also explores complex dynamic behaviour resulting from the coupled nonlinear vibrations.

2. MATHEMATICAL MODEL

The model here presented describes the dynamical behaviour of a drill-string, which considers the axial and torsional degrees-of-freedom, following the ideas presented in Christoforou & Yigit (2003). Besides that, the model aims to describe the non-smooth phenomena associated with these two modes, bit-bounce and stick-slip. The model treats the drill-string as a lumped parameter system, so that the equations are simplified to ordinary differential equations. The forcing comes from the bit-rock interactions, as a result of the string's rotational movement. The

torsional forcing is a result of the friction between bit and rock and the cutting torque acting on the bit. Through a coupling between the equations, the bit interactions with the rock, generate the forcing in axial direction. There is a stiffness associated with the formation, relating the bit penetration into the formation and the axial force exerted.

The model treats the Bottom Hole Assembly (BHA) as a lumped mass at the bottom of the drill-string. The drill-pipes mass is considered as a lumped mass equivalent to its distributed mass. Together, the BHA mass and the equivalent drill-pipe mass make up the axial mass, m_a. The axial displacement is denoted by the x variable. Figure 1 depicts a free body diagram of the system for its axial degree-of-freedom. Figure 1a shows the BHA configuration with the bit hanging just above the formation. In this case the bit exerts zero force on the formation. This point is considered as the origin of the axis, *i.e.* $x = 0$. The x variable is positive when the bit is below $x = 0$. The traction force applied at the top of the BHA, T_1, equals its buoyed weight, P. Figure 1b presents the static equilibrium, with the nominal weight on bit $\underline{F_b}$ applied, but without any rotation of the drill-string. $\underline{F_b}$ is called nominal Weight-On-Bit (WOB) because during the dynamic response of the system this WOB varies. The static displacement, $\underline{x}$, is associated with the drill-bit penetration, when the WOB equals $\underline{F_b}$. As weight is applied on the drill-bit, the traction on top of BHA reduces to the static traction, $\underline{T_2}$,. The traction also varies during the dynamical response. The instantaneous traction and weight are called T_2 and F_b. The torsional degree-of-freedom is analysed by considering that torsional stiffness is provided by the drill-pipes, k_t, in such a way that the BHA does not receive any torsion. The torsional inertia is composed by a combination of a lumped inertia in the tip of the string, associated with the BHA, and the drill-pipes, I_t. Besides, the torsional model assumes a linear viscous damping, c_t. The rotation angle is represented by ϕ.

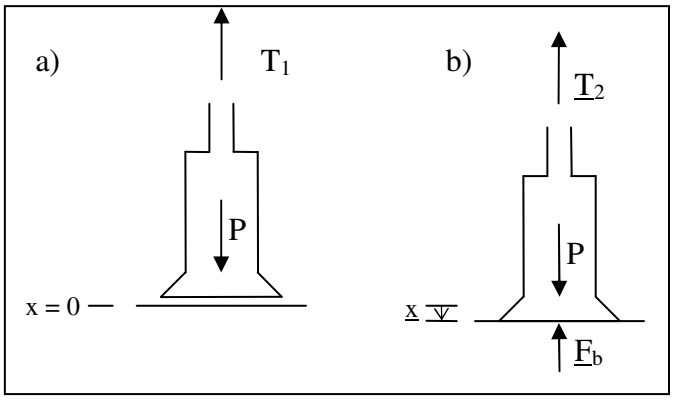

Figure 1 – Free body diagram of the BHA with the axial acting forces.

The equilibrium establishes different conditions related to contact and non-contact behaviour. In general, the governing equation can be written as follows,

$$\begin{cases} m_a \ddot{x} + c_a \dot{x} + k_a x = F_0 - F_b \\ I_t \ddot{\phi} + c_t \dot{\phi} + k_t (\phi - \phi_{mr}) = -T_b \end{cases} \tag{1}$$

where $F_0 = \underline{F_b}\left(1 + \frac{k_a}{k_c}\right)$, and k_a and k_c are respectively, the axial and the formation stiffness; ϕ_{mr} is the rotary table rotation angle. The forces and torques can be defined according the contact or non-contact scenarios as

$$F_b = \begin{cases} k_c \left(x - s_0 \, sen(n_b \phi)\right), & \text{with contact} \\ 0, & \text{without contact} \end{cases} \tag{2}$$

$$T_b = \begin{cases} F_b \left(\frac{2}{3} r_h f(\dot{\phi}) + \varsigma \sqrt{r_h \delta_c}\right), & \text{with contact} \\ 0, & \text{without contact} \end{cases} \tag{3}$$

The coupling between the axial and rotary oscillations is through contact with the formation where the axial force is the catalyst to generate a resistive torque. Specifically, during the contact when drill-bit rotates, n_b is a constant defining how many elevations (peaks) are for one complete bit rotation. For tri-cone bits $n_b = 3$.

The torque acting on the drill-bit is modelled by two terms: the first one related to the dry friction existing between the bit and the formation, and the second one related to the torque needed to cut the rock. The equation proposed Spanos *et al.* (1995) is used where the friction is considered to be evenly distributed on the front face of the bit; r_h is the drill-bit

radius, δ_c is the average cutting depth, ς is a dimensionless parameter that characterizes the force necessary to cut the rock. The average cutting depth, δ_c, is obtained from the following relation:

$$\delta_c = \frac{2\pi TP}{\omega_d} \tag{4}$$

where TP is the average rate of penetration, calculated as a function of the applied weight on bit F_b and the rotary table rotation ω_{mr}, using the following empirical relation:

$$TP = e_1 \underline{F}_b \sqrt{\omega_{mr}} + e_2 \tag{5}$$

where $\underline{F}_b = k_c \underline{x}$, with $\underline{x}$ represents the bit teeth penetration into the formation, when the WOB equals $\underline{F}_b$; e_1 and e_2 are constants.

The dry friction between the formation and the drill-bit introduces one of two non-smoothnesses to the system. This non-smoothness may be treated in a much simpler way than the non-smoothness associated with impacts. That happens because it is relatively simple to define a continuous function of the angular velocity that gets close to the non-smooth shape of the dry friction. That is, a continuous function able to describe both the static and dynamic friction.

The function $f(\dot{\phi})$ defines the dry friction and its sign is always opposite to that of the angular velocity. The function used to $f(\dot{\phi})$ in this work was proposed by Leine (2000):

$$f(\dot{\phi}) = -sign(\dot{\phi}) \left(\frac{2}{\pi}\right) \arctan\left(\varepsilon \dot{\phi}\right) \left(\frac{\mu_e - \mu_d}{1 + \tau \left|\dot{\phi}\right|} + \mu_d \right) \tag{6}$$

In this equation, the constants μ_e and μ_d are the static and dynamic friction coefficients, respectively; ε and τ are dimensionless numerical constants, where $\varepsilon >> 1$ and $\tau > 0$. These constants are responsible for the proper transition from $-\mu_d$ to $+\mu_d$. If properly chosen, these constants can get the smoothened shape of the dry friction really close to that of its original non-smooth function.

Concerning the contact/non-contact non-smoothness, the same procedure used in Savi *et al.* (2007) can be employed in order to smoothness the governing equations. This idea defines a transition region with thickness, η, and under these assumptions, the system is governed by the following equations:

For the situation with contact, where $x \geq s_0 sen(n_b \phi) + \eta$:

$$\begin{cases} m_a \ddot{x} + c_a \dot{x} + k_a x = F_0 - k_c \left(x - s_0\, sen(n_b \phi)\right) \\ I_t \ddot{\phi} + c_t \dot{\phi} + k_t \left(\phi - \phi_{mr}\right) = -k_c \left(x - s_0\, sen(n_b \phi)\right) \left(\frac{2}{3} r_h f\left(\dot{\phi}\right) + \varsigma \sqrt{r_h \delta_c} \right) \end{cases} \tag{7}$$

For the situation without contact, where $x \leq s_0 sen(n_b \phi) - \eta$:

$$\begin{cases} m_a \ddot{x} + c_a \dot{x} + k_a x = F_0 \\ I_t \ddot{\phi} + c_t \dot{\phi} + k_t \left(\phi - \phi_{mr}\right) = 0 \end{cases} \tag{8}$$

For the transition region, where $s_0 sen(n_b \phi) - \eta < x < s_0 sen(n_b \phi) + \eta$:

$$\begin{cases} m_a \ddot{x} + c_a \dot{x} + k_a x = F_0 - \frac{k_c}{2} \left(x - s_0\, sen(n_b \phi) + \eta\right) \\ I_t \ddot{\phi} + c_t \dot{\phi} + k_t \left(\phi - \phi_{mr}\right) = -k_c \left(\frac{2}{3} r_h \eta\, f\left(\dot{\phi}\right) + \varsigma \sqrt{r_h \delta_c}\, \frac{\left(x - s_0\, sen(n_b \phi) + \eta\right)}{2} \right) \end{cases} \tag{9}$$

Many of the system parameters are obtained from the drill-string and drilling fluid characteristics. Thereby, it is important to establish proper equations that allow these parameters to be obtained. Here, parameters are obtained in a similar way to that of Christoforou & Yigit (2003).

3. NUMERICAL SIMULATIONS

In this section numerical results obtained using the proposed model are discussed. Table 1 presents parameters that are used for all simulations (parameters for the rate of penetration, the dry friction smoothening and the transition region). Basically, four different situations are discussed: normal conditions, stick-slip behaviour, bit-bounce behaviour and stick-slip together with bit-bounce behaviour.

Table 1 – Parameters used in simulations.

c_1	c_2	η	τ	ε
-	-	(m)	-	-
1.35×10^{-8}	-1.9×10^{-4}	10^{-6}	10.9	10^{4}

3.1. Normal Conditions

Initially, dynamic responses for normal conditions are computed for the parameters given in Table 2. Figure 2 presents steady state phase portraits for axial and torsional motion. It is a period-1 behaviour that is expected in regular drilling operations, without severe vibrations. Under this condition, discontinuities are not present, which indicates that there is no bit-bounce, and therefore the bit does not loose contact with the formation. Since the angular displacement grows with time, the torsional phase space is monitored by $\phi_{mr} - \phi$. One can deduce that this behaviour is periodic and bounded, which means that the drilling takes place without severe vibration. No occurrence of discontinuities and the fact that the angular velocity is always positive endorse the fact that there is no stick-slip present.

Table 2 – Normal conditions system parameters.

$\underline{F_b}$	ω_{mr}	l_{BHA}	l_{DP}	d_i	d_e	dc_i	dc_e	d_p
(lb)	(RPM)	(m)	(m)	(pol)	(pol)	(pol)	(pol)	(pol)
10000	50	200	700	4	5	3	9	17.5
(kN)	rad/s	-	-	(mm)	(mm)	(mm)	(mm)	(mm)
44.763	5.23599	-	-	101.6	127	76.2	228.6	444.5

ρ_{fl}	μ_{fld}	c_{ma}	c_a	k_f	s_0	n_b	μ_e	μ_d	ς
(lb/gal)	(cP)	-	-	(N/m)	(mm)	-	-	-	-
12.5	200	1.7	4000	25×10^{6}	1	1	0.35	0.3	0.1
kg/m³	Pa.s	-	-	-	-	-	-	-	-
1497.83	0.2	-	-	-	-	-	-	-	-

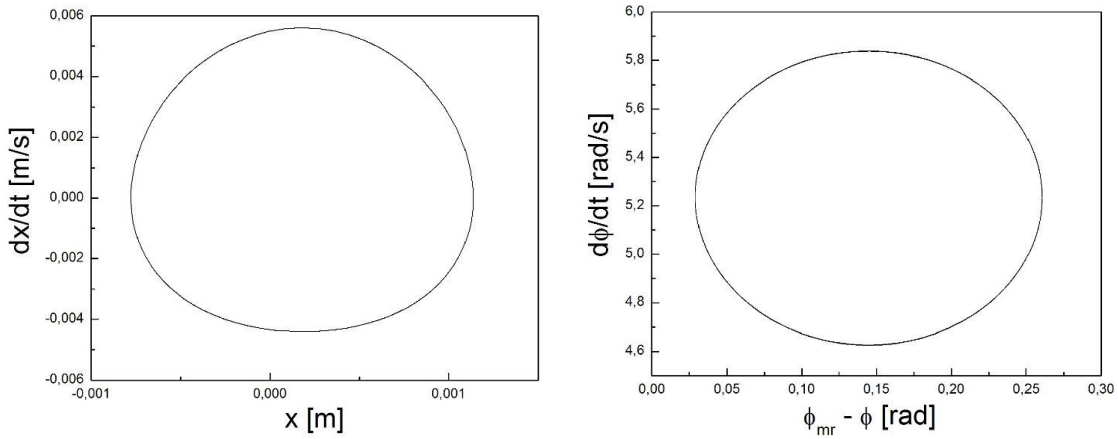

Figure 2 – Phase portraits for axial (left panel) and torsional (right panel) vibrations for the normal conditions.

Figure 3 shows the angular displacement ϕ as a function of time. As the drill-string is continuously rotating, ϕ always increases, fluctuating around ϕ_{mr} value. Figure 3 shows ϕ varying with time and also ϕ_{mr}. One can realize that both curves are almost the same. A more useful way of visualizing the behaviour of ϕ is through the difference between $\phi_{mr} - \phi$ against time. This way what is obtained is the angular distance between the bit and the rotary table. The figure shows how much the rotary table is ahead of the drill-bit, in rad/s.

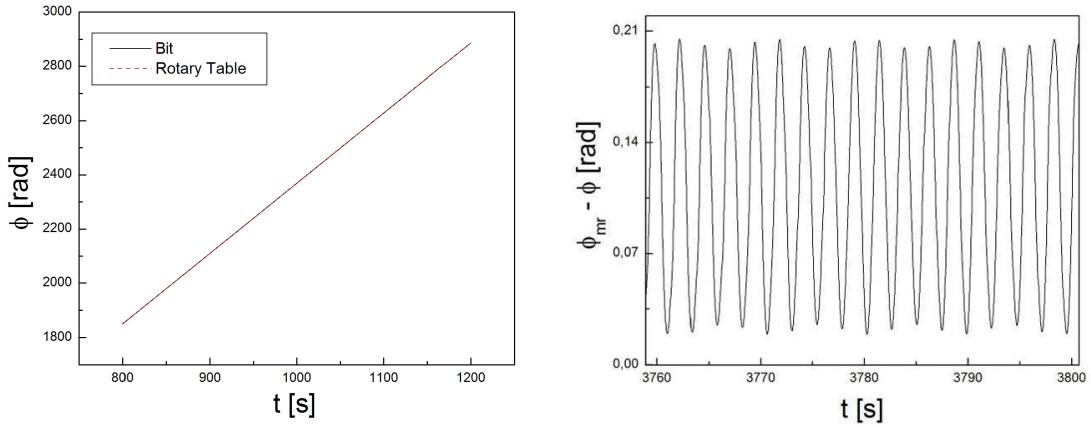

Figure 3 – (left panel) Drill-bit and rotary table angular displacement in time. (right panel) Difference between angular displacement of the drill-bit and rotary table.

3.2. Stick-Slip Behaviour

The stick-slip behaviour is now considered and a new set of parameters is given in Table 3. The only parameters changed with respect to the previous simulation are in the upper table.

Table 3 – Stick-slip system parameters.

F_b	ω_{mr}	l_{BHA}	l_{DP}	d_i	d_e	dc_i	dc_e	d_p
(lb)	(RPM)	(m)	(m)	(pol)	(pol)	(pol)	(pol)	(pol)
15000	30	200	4000	2.764	3.5	2.8125	6.5	26
(kN)	rad/s	-	-	(mm)	(mm)	(mm)	(mm)	(mm)
67.1445	3.14159	-	-	70.2056	88.9	71.4375	165.1	660.4

ρ_{fl}	μ_{fld}	c_{ma}	c_a	k_f	s_0	n_b	μ_e	μ_d	ς
(lb/gal)	(cP)	-	-	(N/m)	(mm)	-	-	-	-
12.5	200	1,7	4000	25×10^6	1.0	1	0.35	0.3	0.1
kg/m³	Pa.s	-	-	-	-	-	-	-	-
1497.83	0.2	-	-	-	-	-	-	-	-

Similarly to Figure 3, Figure 4 also presents phase portraits, however contrary to the previous case a steady state has not been achieved. The angular velocity amplitude increases until it reaches zero velocity (stick). Thereafter, the system behaves with stick-slip. The stick-slip can be clearly seen on the horizontal line present in $d\phi/dt = 0$. The amplitude increase is also noticeable, both in terms of the angular velocity and in the angular displacement, associated with stick-slip. This analysis shows that the phase space is an adequate tool to identify the stick-slip. The axial phase space is also presented in this picture showing a far more intricate steady state behaviour, since the complex torsional behaviour changes the axial behaviour effectively. Despite its complexity, this phase space does not possess any discontinuity whatsoever, indicating that the bit-bounce phenomenon is not taking place.

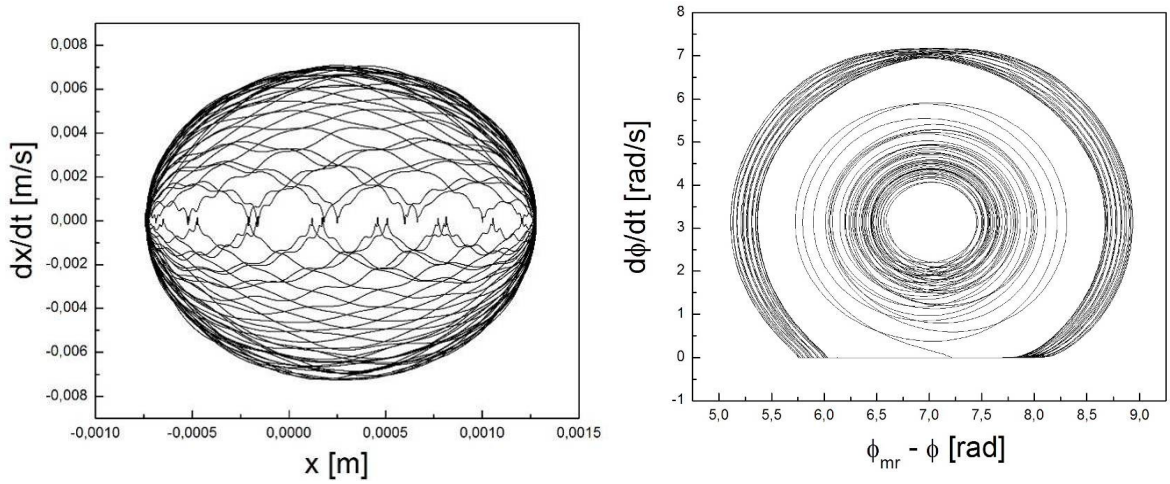

Figure 4 – Phase portraits for axial (left panel) and tortional (right panel) vibrations for the stick-slip case.

Under these conditions, the drilling takes place with the stick-slip behaviour that can be easily observed in Figure 5 that shows the time history of angular velocity $d\phi/dt$. Time intervals in which the angular velocity vanishes can be observed, corresponding to the stick intervals in which the drill-bit stops rotating. It is hard to compare the velocity peaks of this result with those of the previous one because many parameters are really different. Nevertheless, a qualitative comparison can be made observing the forcing frequencies (the rotary table angular velocity) in each case. In the previous simulation, $\omega_{mr} = 5.236$ rad/s and the peaks of $d\phi/dt$ reach about 5.8 rad/s, which is just above the forcing frequency. In this second case, on the other hand, $\omega_{mr} = 3.14$ rad/s and the peaks of $d\phi/dt$ is about 7.0 rad/s, which is far above the forcing frequency. Therefore, it is possible to conclude that when stick-slip is present, the drill-bit exhibits high amplitude peaks, what could explain the strong drill-bit wear usually related to this kind of response. In order to understand this phenomenon, one should observe whether there is stick-slip or not, the average angular velocity of the bit should be, in the long term, very close to that of the rotary table. Hence, when stick-slip is present there are periods during which the drill-bit angular velocity vanishes, and this must be compensated with periods in which the drill-bit velocity is far above the one of the rotary table's; so in this way the average is maintained. Figure 5 also presents the time history of $\phi_{mr} - \phi$. This picture allows one to observe that an angular distance between the drill-bit and rotary table

oscillates around approximately 7 rad, which corresponds to a little bit more than a complete turn. Besides, this movement amplitude varies about 1.7 rad around this average value. In the previous case, the average was around 0.11 rad, and the amplitude around 0.08 rad. This larger distance between the drill-bit and rotary table is probably not due to the stick-slip, but to the fact that the drill-string used in this case has a lower stiffness. That occurs because it is composed of smaller diameter drill-pipes and it is much longer. The large fluctuations of $\phi_{mr} - \phi$, on the other hand, may be related to the stick-slip. During the stick phase the rotary table keeps on turning while the bit is standing still, and that brings both far apart. Another interesting conclusion is that stick-slip is not easily identifiable through the analysis of the angular displacement. Therefore, to identify this behaviour it is more adequate to analyse the angular velocity or the phase space, as presented as follows.

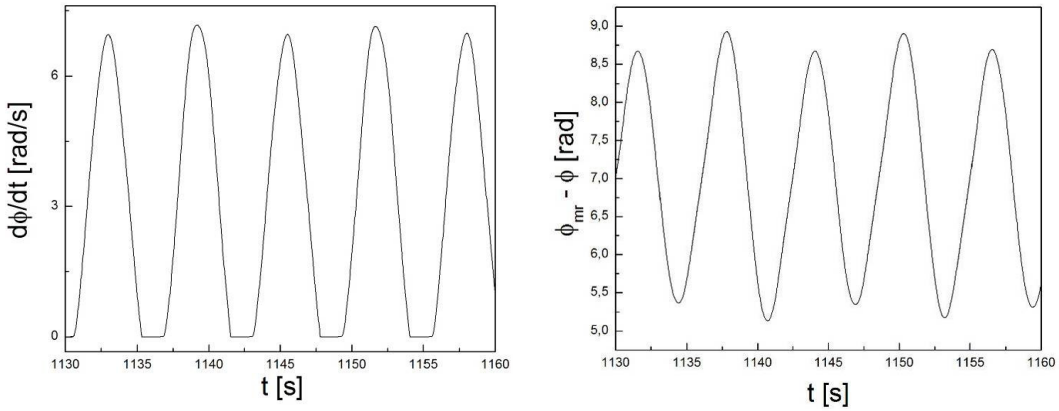

Figure 5 – Time histories of angular displacement (left panel) and relative angular displacement (right panel)

Another interesting observation is that the stick phases alternates between low and high values of x. That is due to the elevation existing in the formation, ahead of the drill-bit, characterized by the s_0 parameter. The confirmation to this explanation can be made from the fact that the time interval between two consecutive sticks is about 5s. As the rotary table rotation is 30 rpm, that is one rotation every 2 s, that means there is one stick every 2.5 rotations, approximately.

3.3. Bit-Bounce Behaviour

The bit-bounce behaviour is now in focus by having a new set of parameters presented in Table 4. Once again, there are changes only on the upper table values, compared to the previous set of parameters.

Table 4 – Bit-bounce system parameters.

F_b	ω_{mr}	l_{BHA}	l_{DP}	d_i	d_e	dc_i	dc_e	d_p
(lb)	(RPM)	(m)	(m)	(pol)	(pol)	(pol)	(pol)	(pol)
5000	70	200	5000	2.764	3.5	2.8125	6.5	17.5
(kN)	rad/s	-	-	(mm)	(mm)	(mm)	(mm)	(mm)
22.3815	7.33038	-	-	70.2056	88.9	71.4375	165.1	444.5

ρ_{fl}	μ_{fld}	c_{ma}	c_a	k_f	s_0	n_b	μ_e	μ_d	ς
(lb/gal)	(cP)	-	-	(N/m)	(mm)	-	-	-	-
12.5	200	1.7	4000	25×10^6	1	1	0.35	0.3	0.1
kg/m³	Pa.s	-	-	-	-	-	-	-	-
1497.83	0.2	-	-	-	-	-	-	-	-

Figure 6 shows the axial phase portrait where the behaviour is quite different from the others, since a bit-bounce is observed. The system response is clearly divided in two distinct regions, highlighting the non-smoothness related to the bit-bounce. It can be clearly seen that the displacement is much greater than in the previous cases, despite the fact that

the parameters have not been changed too much. The surface elevation (s_0), just like before, is 1mm, and the displacement now reach values on the order of 40mm, what gives a clear evidence that the contact has been lost.

By looking at the torsional phase portrait, one can see that there is no apparent stick-slip but, in a similar way to what the stick-slip did to the axial phase portrait, the bit-bounce has turned the torsional behaviour to much more complex. The orbits seen fill the phase space, but the behaviour should not be confused with a chaotic motion. It is interesting to point out that, unlike what happens during the stick-slip, when the torsional mode discontinuity cannot be seen on the axial phase space, here the axial mode discontinuity can be seen on the torsional phase space.

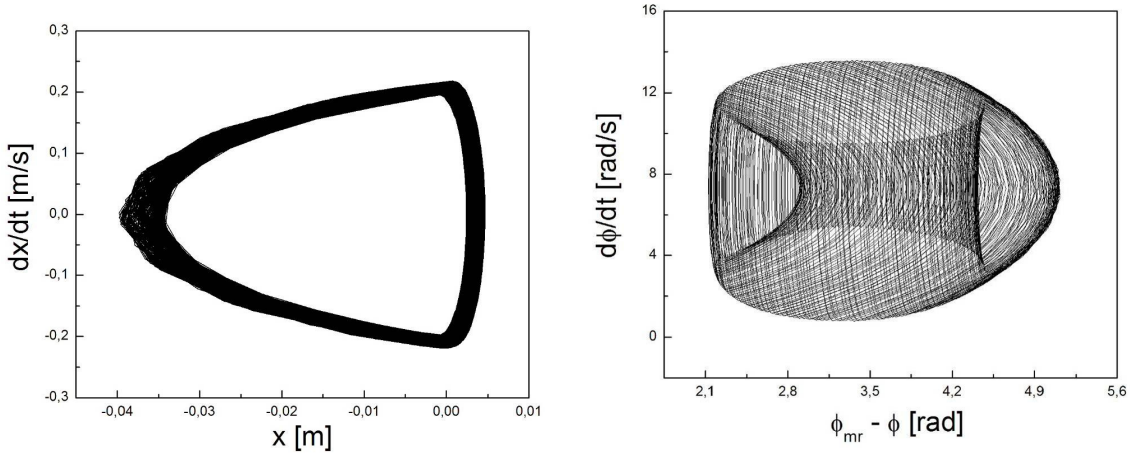

Figure 6 – Phase portraits for axial (left panel) and torsional (right panel) vibrations for the bit-bounce case.

Figure 7 shows the axial displacement and the axial velocity time histories. Comparing to the first case, for which had steady state vibrations, it can be observed that the responses are less smooth and having sharper peaks. However, it is not easy to realize the bit-bounce existence through these graphs.

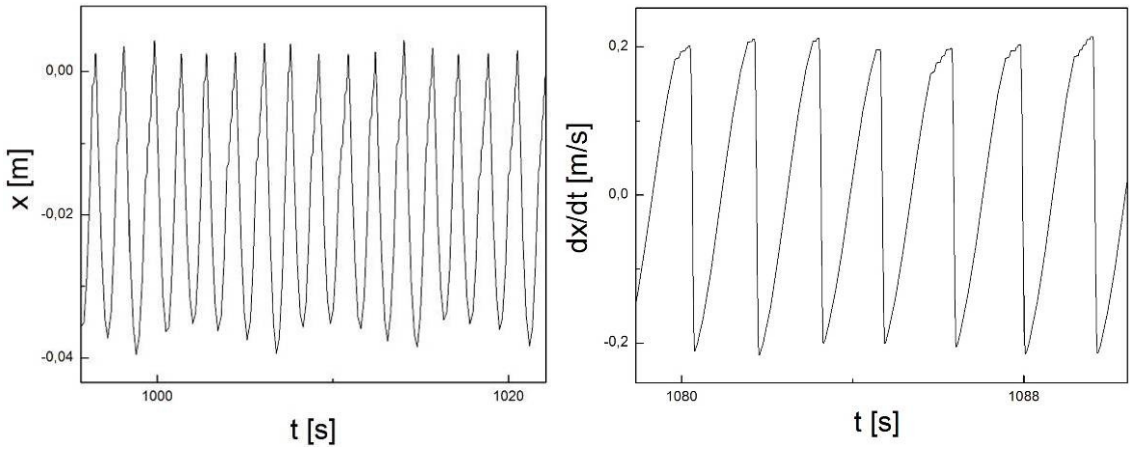

Figure 7 – Time histories of axial displacement (left panel) and velocity (right panel)

3.4. Stick-Slip and Bit-Bounce Behaviours

At this point, friction coefficients are altered in order to investigate a case where stick-slip and bit-bounce behaviours occur simultaneously. Table 5 gives the system parameters for this situation.

Table 5 – System parameters for stick-slip and bit-bounce behavior.

$\underline{F_b}$	ω_{mr}	l_{BHA}	l_{DP}	d_i	d_e	dc_i	dc_e	d_p
(lb)	(RPM)	(m)	(m)	(pol)	(pol)	(pol)	(pol)	(pol)
5000	70	200	5000	2.764	3.5	2.8125	6.5	17.5
(kN)	rad/s	-	-	(mm)	(mm)	(mm)	(mm)	(mm)
22.3815	7.33038	-	-	70.2056	88.9	71.4375	165.1	444.5

ρ_{fl}	μ_{fld}	c_{ma}	c_a	k_f	s_0	n_b	μ_e	μ_d	ς
(lb/gal)	(cP)	-	-	(N/m)	(mm)	-	-	-	-
12.5	200	1.7	4000	25×10^6	1.0	1	0.6	0.5	0.1
kg/m³	Pa.s	-	-	-	-	-	-	-	-
1497.83	0.2	-	-	-	-	-	-	-	-

The axial phase portrait depicted in Figure 8a shows the presence of the bit-bounce phenomenon. This conclusion is taken from the existence of two distinct regions, indicating the non-smoothness characteristic of this phenomenon. Figure 8b shows the torsional phase space, where one can find points with zero velocity. Here, it is possible to indentify both behaviours from phase spaces.

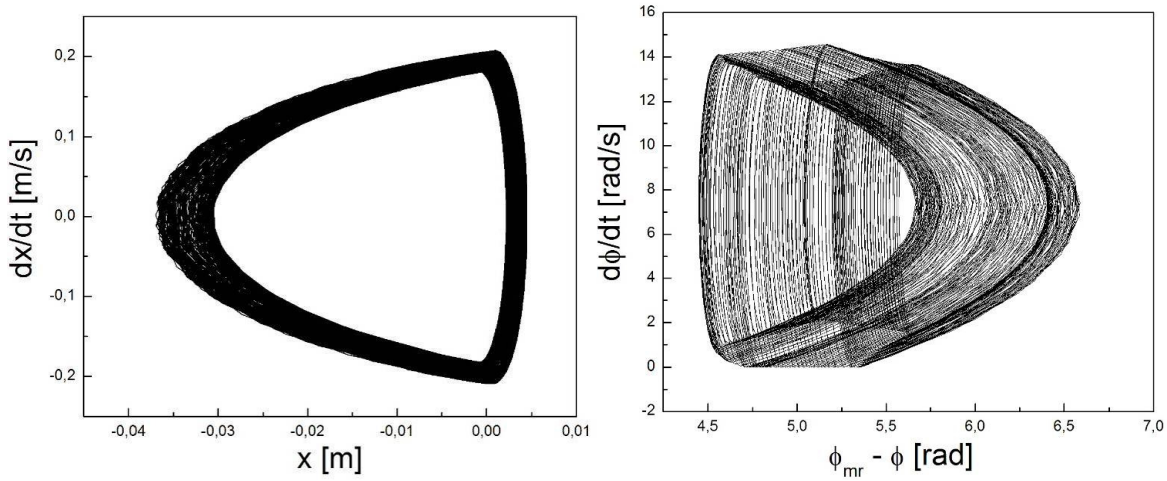

Figure 8 – Phase portraits for axial (left panel) and torsional (right panel) vibrations for the stick-slip and bit-bounce case.

4. CONCLUSIONS

In this paper, we model and analyse drill-string vibrations with respect to two fundamental phenomena: stick-slip and bit-bounce. These behaviours are responsible for most of damages of the drill-strings and drill-bits being important to be identified. We built a two degree-of-freedom model to account for axial and torsional vibration. The coupling between both vibration modes is through contact with the formation where the axial force is the catalyst to generate a resistive torque. The forces and torques are defined according the contact or non-contact scenarios, establishing a non-smooth system. Besides, the dry friction between the formation and the drill-bit introduces another non-smoothness to the system. The resulting non-smooth system is treated by promoting the smoothness of the governing equations. We adopt smooth functions which are advantageous in terms of mathematical description and numerical analysis. A special attention is given to the transitions between different phases of motion, which for stick-slip and bit-bounce are normally treated as the non-smooth dynamics. Based on this procedure, numerical simulations are carried out showing different kinds of response. Basically, four situations are of concern: normal condition; stick-slip behaviour; bit-bounce behaviour; stick-slip and bit-bounce simultaneously. Our studies have showed that the developed mathematical model is capable of predicting a full range of dynamic responses including the non-smooth behaviour.

5. ACKNOWLEDGEMENTS

The authors would like to acknowledge the support of the Brazilian Research Agencies CNPq and FAPERJ and through the INCT-EIE (National Institute of Science and Technology - Smart Structures in Engineering) the CNPq and FAPEMIG. The Air Force Office of Scientific Research (AFOSR) is also acknowledged.

6. REFERENCES

Andreaus, U. & Casini, P., 2001, "Dynamics of Friction Oscillators Excited by a Moving Base and/or Driving Force", *Journal of Sound and Vibration*, v.245, n.4, pp.685-699.

Christoforou, A. P. & Yigit, A. S., 2003, "Fully Coupled Vibrations of Actively Controlled Drillstrings", *Journal of Sound and Vibration*, v.267, pp.1029-1045.

Franca, L. F. P. & Weber, H.I., 2004, "Experimental and Numerical Study of a New Resonance Hammer Drilling Model with Drift", *Chaos, Solitons and Fractals*, v.21, pp.789–801.

Hinrichs, N., Oestreich, M. & Popp, K., 1998, "On the Modelling of Friction Oscillators", *Journal of Sound and Vibration*, v.216 (3), pp.435-459.

Leine, R.I., 2000, "*Bifurcations in Discontinuous Mechanical Systems of Filippov-Type*", Ph.D. Thesis, Technische Universiteit Eindhoven.

Pavlovskaia, E., Wiercigroch, M. & Grebogi, C., 2001, "Modeling of an Impact System with a Drift", *Physical Review E*, v.64, 056224.

Savi, M.A., Divenyi, S., Franca, L.F.P. & Weber, H.I., 2007, "Numerical and Experimental Investigations of the Nonlinear Dynamics and Chaos in Non-Smooth Systems with Discontinuous Support", *Journal of Sound and Vibrations*, v.301, pp.59-73.

Silveira, M. & Wiercigroch, M., 2009, "Low Dimensional Models for Stick-Slip Vibration of Drill-Strings", *Journal of Physics: Conference Series*, v.181, 012056.

Spanos, P. D., Sengupta, A. K., Cunningham, R. A. & Paslay, P. R., 1995, "Modelling of Roller Cone Bit Lift-off Dynamics in Rotary Drilling", *ASME Journal of Energy Resources Technology*, v.117, pp. 197-207.

Wiercigroch, M., 2000, "Modelling of Dynamical Systems with Motion Dependent Discontinuities", *Chaos, Solitons and Fractals*, v.11, pp.2429-2442.

7. RESPONSIBILITY NOTICE

The author(s) is (are) the only responsible for the printed material included in this paper.